Mono- and Di-nitroalkyl-(cycloalkyl-)pyrenes in Superacid Media: Dihydroxyiminium-(oxoiminium-)pyrenium Dications; Cyclisation to Long-lived Oxazoline- (and 1,2-oxazine-)pyrenium Ions, Ring Opening to form Nitrosoalkylpyrenium and Nitroso Radical Cation Salts with Unprecedented Stability

Kenneth K. Laali,*[,a] Simon Bolvig[b] and Poul Erik Hansen*[,b]
[a] *Department of Chemistry, Kent State University, Kent, OH 44242, USA*
[b] *Department of Life Sciences and Chemistry, Roskilde University, PO Box 240, DK-4000 Roskilde, Denmark*

The low temperature protonations of sterically crowded molecules 2,4,6,8,10-pentaisopropyl-1-nitropyrene **1**, 2,4,6,8,10-pentaisopropyl-1,3-dinitropyrene **12**, 3,6,8,10-tetracyclohexyl-1-nitropyrene **16**, 2,7-di-*tert*-butyl-1-nitropyrene **19**, 2,7-di-*tert*-butyl-1,8-dinitropyrene **21**, 1,3,6,8-tetraisopropyl-4-nitropyrene **23** and parent 1-nitropyrene **28**, all possessing buttressed nitro groups, were studied in various superacid media under persistent ion conditions. Nitro group diprotonation was observed in all cases to give *N,N*-dihydroxyiminium–pyrenium (or oxoiminium–pyrenium) dications. The resulting dications derived from **1**, **12**, **16** and **23** undergo a facile intramolecular nitro group cyclisation (which is usually complete within minutes at −75 °C ⟶ room temp.) to give oxazoline-(or oxazine-)pyrenium cations **6** (and **11**), **14** (and **15**), **18** and **25**. The charge distribution patterns (probed by ^{13}C and ^{1}H chemical shift analysis) for the iminium–pyrenium dications and their cyclised derivatives illustrate extensive charge delocalisation away from the iminium group at the alternating carbons of the periphery, similar to alkylpyrenium and fluoro(alkyl)pyrenium ions. The remote α positions carry substantial positive charge, which increases with the presence of inductively stabilising alkyl (cycloalkyl) substituents. The assignment of the iminium carbon was proved by independent synthesis and protonation of the 15-N labelled **1**. Quenching of **6**, **18** and **14** (containing **15**) does not furnish their *N*-hydroxyoxazoline derivatives (like **5**) nor the alkylnitropyrene precursors. Instead, the corresponding nitroso-alkylpyrenium and its derived radical cation salts (like **9a** and **9RC**) are obtained (EPR), which when re-dissolved in CF_3SO_3H or FSO_3H reform the cyclised pyrenium ions. Formation of persistent radical cations was also detected in some cases upon storage of the nitroalkylpyrene samples in CF_3SO_3H ('TfOH') at room temperature.

Ring opening of **25** and reduction upon quenching produces a different type of persistent nitrosoalkylpyrene radical (**27** ⟷ **27a**) with smaller a_N. The mechanistic aspects of nitro group cyclisation/ring opening are discussed.

Early work of Gillespie[1] and Deno[2] on protonation of nitrobenzenes in sulfuric acid and oleum and subsequent stable ion studies of Olah and co-workers[3] in higher H_0 superacids have established that in the benzene series the nitro group is protonated and arenium ions are not formed. A similar conclusion was reached in methylation and Lewis acid complexation of nitrobenzenes.[4] On the other hand, the *para*-substituted nitrosobenzenes are *N,O*-diprotonated, forming persistent *N*-hydroxyiminium–benzenium dications.[5]

The same intermediate was postulated in arylation of nitrosobenzene (and nitrobenzene) using CF_3SO_3H (TfOH).[6] Diprotonation of 1-nitronaphthalene at the nitro group with TfOH and formation of a room temperature stable *N,N*-dihydroxyiminium–naphthalenium dication has also been reported.[7]

Whereas the formation of an oxoiminium–naphthalenium dication was considered by Shudo,[6] it was ruled out based on quenching experiments with ^{18}O-labelled water. The importance of a *N,N*-dihydroxyiminium ion intermediate has also been shown in protonation of aliphatic nitro derivatives with TfOH by Jacquesy *et al.*,[8–11] pointing to protonated nitronic acid as a precursor to hydroxy–nitrilium ion, the trapping of which with arenes gave oximes.

As part of a broader study on nitration of sterically congested alkylpyrenes and protonation/transfer-nitration chemistry of the resulting buttressed nitroarenes,[12] we reported that 2,4,6,8,10-pentaisopropyl-1-nitropyrene **1** and 2,4,6,8,10-pentaisopropyl-1,3-dinitropyrene **12**, accessible by classical protic nitration of pentaisopropylpyrene, are diprotonated at a nitro group in TfOH–SO_2 to give persistent *N,N*-dihydroxyiminium–pyrenium dications **2** and **13**. The less buttressed 1-nitropyrene **28** is similarly NO_2-diprotonated (in 1:1 FSO_3H·SbF_5–SO_2), but the planar 2-nitropyrene **30** was found to be ring protonated.[12]

We noted a very facile nitro group cyclisation (**2** ⟶ **6**; Scheme 1). The NO_2 cyclisation had been previously observed by Shudo *et al.*,[13] for 2-cyclopropyl-1-nitrobenzene–TfOH, and by Ridd and associates[14] with 1,3-dialkyl- (or *ortho*-monoalkyl) 2-nitrobenzene–TfOH systems. In the latter, the corresponding anthranils (2,1-benzisoxazoles) were isolated by reaction of 1-ethyl- and 1,3-diethyl-2-nitrobenzene with TfOH at *ca.* 100 °C, whereas with 1-methyl-2-nitrobenzene little anthranil could be seen. Involvement of the *aci* form was postulated.[14a] It appears that steric crowding in the *ortho* position facilitates cyclisation. Subsequent deuterium labelling studies favoured an intramolecular H-transfer process (a [1,5]-sigmatropic H-shift).[15a]

2-Nitrobenzyl alcohol reacts with TfOH at 90 °C to give 4-amino-3-carboxylphenyl triflate *via* the C-protonated conjugate acid of anthranil *N*-oxide.[15b]

In order to test the generality and scope of nitro group cyclisation, we have synthesised model compounds with nitro

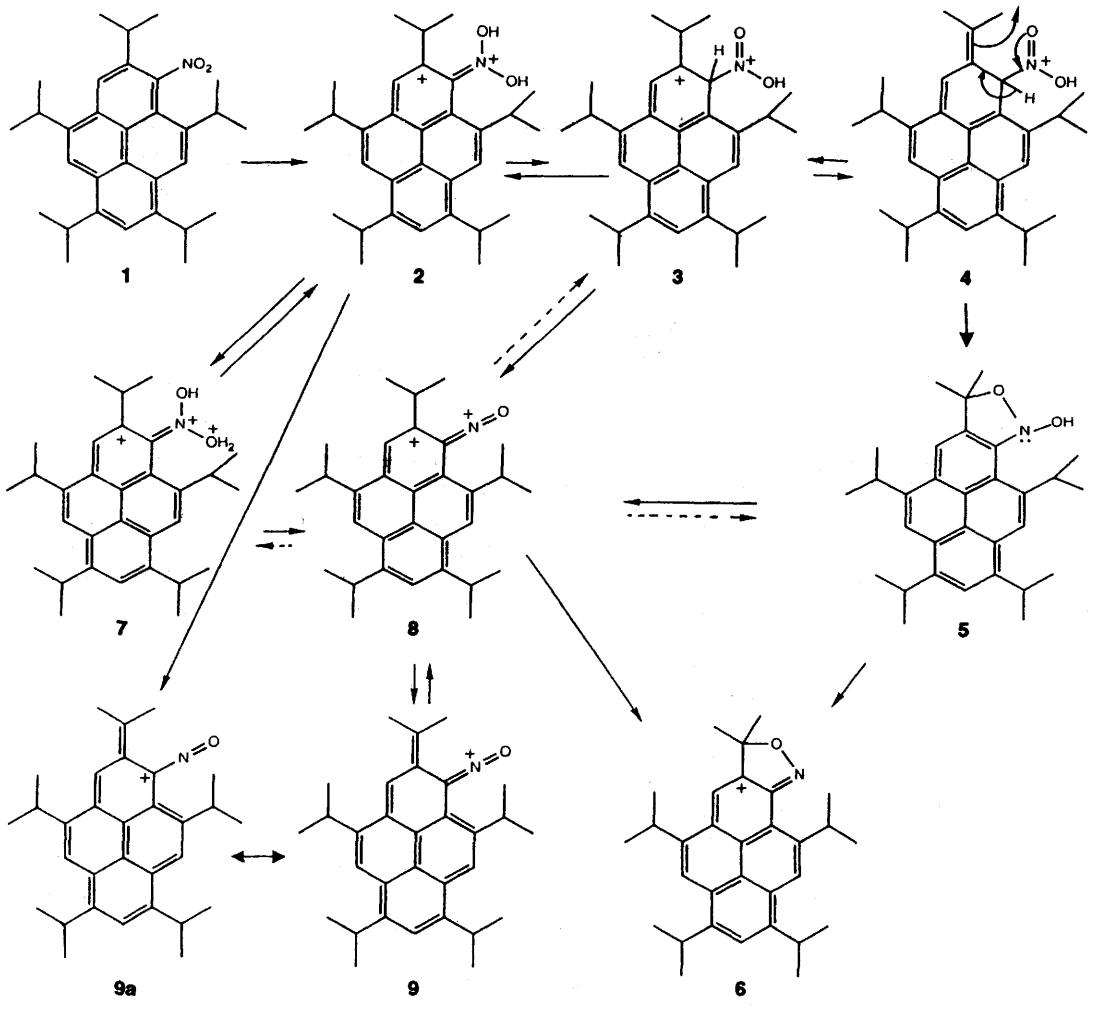

Scheme 1 Protonation and cyclisation of 2,4,6,8,10-pentaisopropyl-1-nitropyrene (**1**). The counterions are not given in the schemes, but are usually fluorosulfates.

groups strategically positioned in highly buttressed environments (*peri* and *ortho* strain).

With **1**, the extreme facility of the cyclisation process (within minutes at −75 °C ⟶ room temp.) suggested possible synthetic utility to make oxazoline (or oxazine) derivatives of PAHs in one-pot procedures. Moreover, our suggested mechanism [12] requires the presence of at least one hydrogen at the α carbon of the side chain for cyclisation to occur. Bulky *tert*-butyl groups placed in the β position in α-nitropyrenes are ideally suited for this test as they provide *ortho* strain with immunity to Bu^t disproportionation in the superacid due to very unfavourable energetics of the σ complex of β attack.[16]

The present study focuses on the scope and generality of iminium–pyrenium dication formation in a series of buttressed nitropolyalkylpyrenes: 2,4,6,8-tetraisopropyl-1-nitropyrene **1**, 2,4,6,8-tetraisopropyl-1,3-dinitropyrene **12**, 3,6,8,10-tetracyclohexyl-1-nitropyrene **16**, 2,7-di-*tert*-butyl-1-nitropyrene **19**, 2,7-di-*tert*-butyl-1,8-dinitropyrene **21** and 1,3,6,8-tetraisopropyl-4-nitropyrene **23**. In addition, the parent compound 1-nitropyrene **28** was reinvestigated.

In order to determine the influence of the iminium cation moiety on the charge distribution mode, we carried out detailed NMR studies (^{13}C, ^{1}H and H–C HETCOR) on the dihydroxyiminium(oxoiminium)–pyrenium dications and their cyclised cations. The data are gathered in Figs. 1 and 2 and in Tables 1 and 2. These findings are compared with our previous studies of alkyl(cycloalkyl)pyrenium [16] and fluoro(alkyl)-pyrenium [17] ions of protonation. Diprotonation of the 15-N labelled **1** allowed the unambiguous assignment of the iminium carbons in **2** and **6**.

Assignment of NMR Spectra.—^{1}H *NMR spectra.* The ^{1}H NMR spectra were assigned based on protonation shifts.[17,18] The 3-H (*meta*) resonance is shifted to high field, whereas all other resonances are shifted to low field (Table 1). Furthermore, the $^3J(H_{\alpha\beta},H_{\alpha\beta})$ coupling is greatly reduced in the pyrenium ions.

^{13}C *NMR spectra.* The ^{13}C NMR spectra of the precursors were assigned based on substituent effects of simple nitro-compounds paired with intensity observations. The observation of one-bond and long-range carbon–nitrogen couplings and the one-bond ^{15}N isotope effects on ^{13}C chemical shifts were of great help in assigning the carbons close to the nitro group of **1** and **28**. The latter assignment is slightly different from that given in ref. 19. Multiplicities due to C–H couplings of **19** and **20** are known.[20] The substituent effect of the nitro group is seen to be smallest for the unsubstituted compound **28**. The assignment of the ^{13}C spectrum of **12** reveals a considerable high field shifts of C-4, C-10 and C-3a, C-10a, also seen to a lesser extent for C-10, C-10a in the spectra of **1** and **28** (Table 2).

The assignments of the protonated nitropyrenes are in general based on substituent effects, comparison of chemical shifts of similar compounds, HETCOR and off resonance decoupling experiments. For **2** and **6** the one-bond carbon–nitrogen coupling constant and the ^{15}N one-bond isotope effect identified the C-1 unambiguously. The high field shift of the *peri*

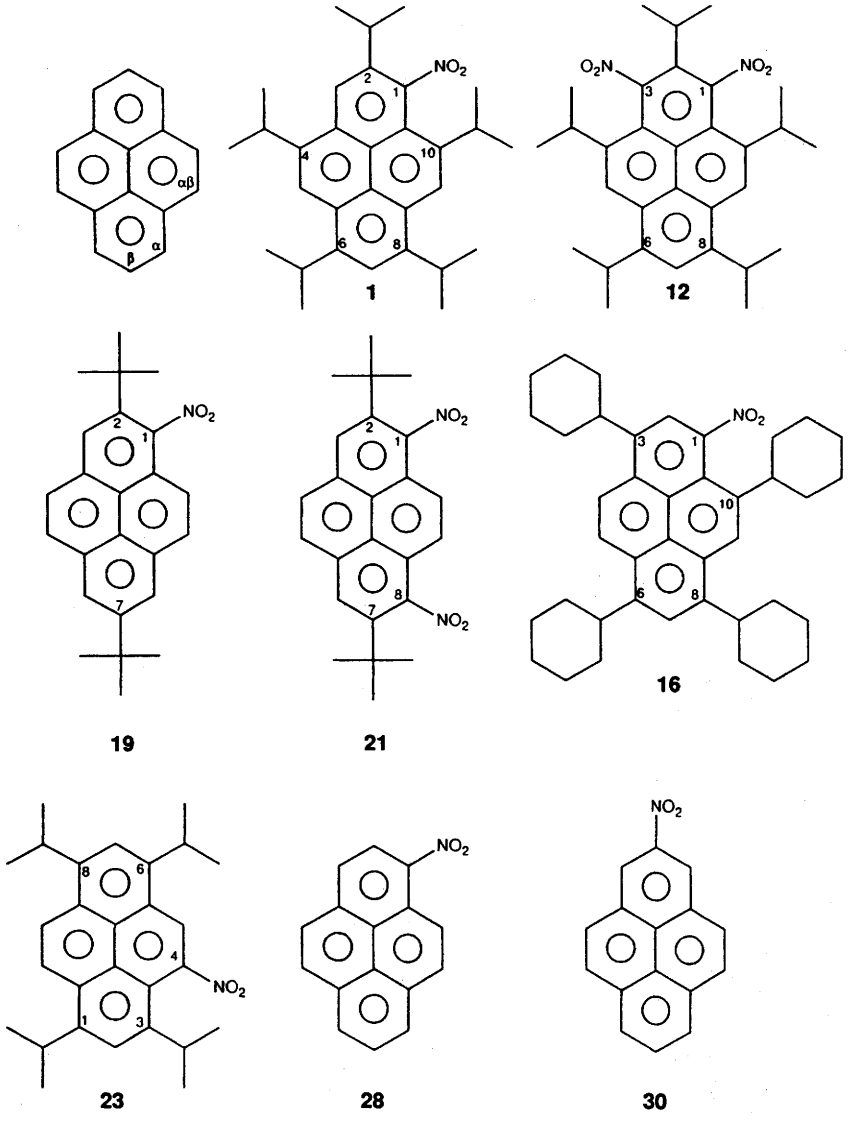

carbon is also observed in **2**, **6**, **13**, **14**, **17** and **18**, but not in the other two α-substituted ions, **20** and **29**. Several of the protonated species have been investigated in both SO_2ClF and SO_2 co-solvents and in various superacid media. For **2**, a clear solvent dependence could be established (Fig. 2). For **20** a chemical shift difference is also observed with SbF_5 containing superacids (Fig. 2).

Results and Discussion

Protonation of **1** *with* TfOH–SO_2 *and* FSO_3H·SbF_5 (4:1)–SO_2ClF *and Subsequent Cyclisation*.—Compound **1** reacted with TfOH–SO_2 at dry ice–acetone temperature to give **2** as the only observable cation [^{1}H NMR; Fig. 3(*a*)]. Similar spectra were obtained in FSO_3H–SO_2 or in FSO_3H–SO_2ClF solvents. Complete cyclisation (⟶ **6**) occurs rapidly when the sample temperature is allowed to increase slowly to ambient (slow evaporation of SO_2 in a stream of dry nitrogen). Thus the ^{1}H NMR spectrum of the sample after *ca.* 5 min following re-cooling and addition of fresh liquid SO_2 showed only **6** [Fig. 3(*b*)]. The energy barrier to cyclisation must be quite low, since in samples prepared with higher substrate:TfOH ratios for ^{13}C NMR studies, the rearranged cation was already present as a minor product, presumably due to increased local overheating.

Careful preparation at −75 °C either with TfOH–SO_2, FSO_3H–SO_2 (or SO_2ClF), or in the higher acidity superacid FSO_3H·SbF_5 (4:1)–SO_2ClF ensures clean formation of **2** free of **6**.

The onset of cyclisation (⟶ **6**) is easily detectable as the characteristic deshielded methyl singlet at δ 2.06 appears in the ^{1}H NMR spectrum with concomitant appearance of four new deshielded aromatic singlets [Fig. 3(*b*)].

The aliphatic regions of the ^{1}H NMR spectra of **2** and **6** deserve comment. The Pr^i(Me) region for **2** [Fig. 3(*a*)] comprises five doublets between 1.37–1.75 ppm, whereas for **6** there are just three Pr^i(Me) doublets (2:1:1) between 1.46–1.59 ppm with the two most upfield ones overlapping. The two anisotropically shielded methyl doublets in **2** must logically be one *peri* and one *ortho* relative to the diprotonated nitro group. Absence of any significant anisotropic shielding of the *peri* Pr^i(Me) in the oxazoline–pyrenium cation **6** and its presence in **2** may be taken as indirect evidence for the presence of the OH groups in the latter, whose protons are not observable as separate signals in the TfOH–SO_2 system nor in FSO_3H·SbF_5 (4:1)–SO_2ClF, presumably still due to a rapid exchange process (see later discussion). The NMR data in TfOH–SO_2 or in FSO_3H·SbF_5 (4:1)–SO_2ClF appear more compatible with a dihydroxyiminium–pyrenium species, **2** than an oxoiminium–pyrenium dication **8**.[12]

The Pr^i(CH) multiplets of **2** are between δ 3.23–4.24. Upon

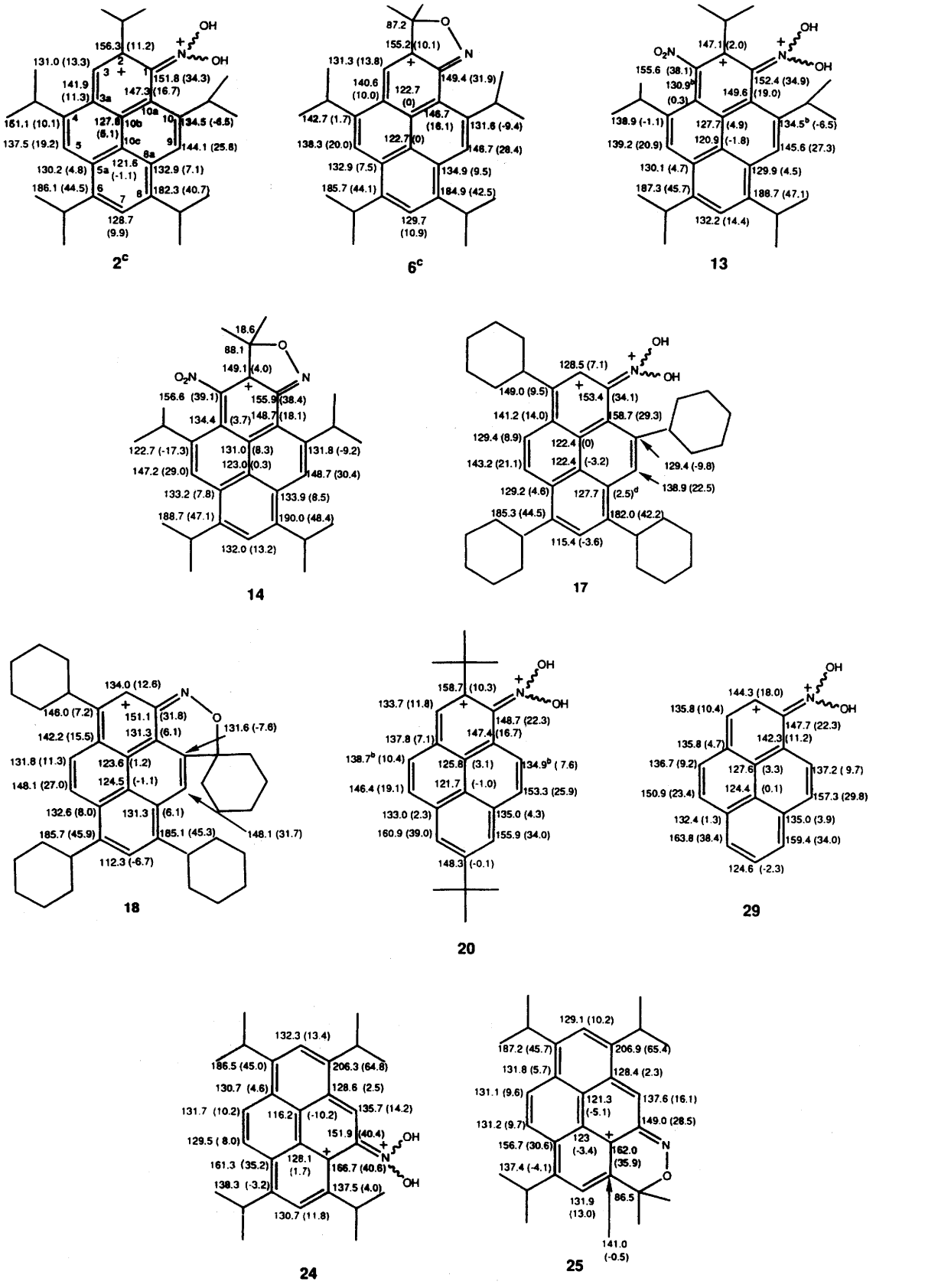

Fig. 1 ^{13}C chemical shifts and $\Delta\delta$ values.[a] Solvent FSO_3H–SO_2. [a] Relative to parent hydrocarbons. [b] May possibly be exchanged. [c] Solvent CF_3SO_3H–SO_2. [d] Assignment tentative.

cyclisation (⟶ **6**) the most shielded Pr^i(CH) disappears; only three Pr^i(CH) multiplets (in a 2:1:1 ratio) are seen. Thus the shielded 3.21 ppm multiplet reflects buttressing, anisotropic shielding and ring current effects.

The ^{13}C NMR spectrum of **2** [Fig. 4(*a*)] exhibits sixteen aromatic absorptions between δ 187.5–122.3, those at 144.7, 137.8, 132.8 and 129.2 are hydrogen-bearing (HETCOR analysis). Unambiguous assignment of the iminium carbon at δ

Table 1 ^{1}H NMR chemical shifts of protonated and parent nitropyrenes[a]

	Solvent	2-H	3-H	4-H	5-H	6-H	7-H	8-H	9-H
2	CF_3SO_3H–SO_2[b]	—	7.48	—	9.05[d]	—	7.98	—	8.95[d]
6	CF_3SO_3H–SO_2[b]	—	8.16[d]	—	9.19	—	8.37[d]	—	9.30
13	FSO_3H–SO_2	—	—	—	9.10[d]	—	8.13	—	9.16[d]
14	FSO_3H–SO_2	—	—	—	9.32[d]	—	8.25	—	9.42[d]
17	FSO_3H–SO_2ClF	7.25	—	8.35 (7.8)	9.20 (7.8)	—	8.08	—	9.06
18	FSO_3H–SO_2ClF	7.60	—	8.63 (~8.6)	9.47 (~8.6)	—	8.22	—	9.41
20	CF_3SO_3H–SO_2[g]	—	7.68	8.06 (7.8)	8.91 (7.8)[h]	9.16[d]	—	8.93[d]	9.50[d] (8.2)
20	FSO_3H–SbF_5 (1:1)–SO_2	—	7.53	7.97	8.70	8.96	—	9.10	8.91
22[i]	CF_3SO_3H–SO_2	—	7.84	8.21 (7.9)[m]	9.12 (7.9)	9.52	—	—	9.54[j]
23	$CDCl_3$	7.46 (10.0)	7.97 (10.1)	8.28	9.19	9.10	8.27	9.10	9.19
24[k]	CF_3SO_3H–SO_2	9.05	—	—	7.66	—	7.75	—	8.47 (s)
25[k]	CF_3SO_3H–SO_2	8.97	—	—	7.82[d]	—	7.84[d]	—	8.61 (s)
16	$CDCl_3$	8.38	—	8.31 (9.70)	8.49 (9.70)	—	7.97	—	8.08
19[m]	$CDCl_3$	—	8.25	8.08	7.97	8.25	—	8.23	7.70
21[m]	$CDCl_3$	—	8.37	8.10	8.10	8.37	—	—	7.84

	10-H	Aliphatic
2	—	4.23 (CH-6/8), 3.63 (CH-4), 3.52 (CH-10), 3.21 (CH-2), 1.53 (CH_3-6/8), 1.44 (CH_3-4), 1.62, 1.25 (CH_3-2), 1.33, 1.44 (CH_3-10)[c]
6	—	4.30 (CH-6/8), 3.87 (CH-10), 3.83 (CH-4), 2.15 (CH_3-2), 1.68 (CH_3-6/8), 1.63 (CH_3-10), 1.60 (CH_3-4)
13	—	4.32 (CH-6/8), 3.08 (CH-4/10), 3.08 (CH-2), 1.70, 1.36 (CH_3-2)[f], 1.60 (CH_3-4/6/8)[e], 1.43, 1.53 (CH_3-10)[f]
14	—	4.35 (CH-6/8), 3.30 (CH-10), 3.19 (CH-4), 2.16 (CH_3-2), 1.65 (CH_3-8)[d], 1.63 (CH_3-6)[d], 1.57 (CH_3-10)[d], 1.45 (CH_3-4)[d]
17	—	3.90 (CH-6/8), 3.15 (CH-3), 2.83 (CH-10), 2–1.0 (m)
18	—	3.90 (CH-6/8), 3.40 (CH-3), 2.60, 2.38 (CH_2-9), 2.2–1.4 (m)
20	9.07[d] (8.3)	1.56 (CH_3-2), 1.47 (CH_3-7)
20	8.76	1.53 (CH_3-2/7)
22[i]	8.60[j]	1.66 (CH_3-7), 1.56 (CH_3-2)
23	—	—
24[k]	8.47(s)	4.14 (CH-8), 3.69 (CH-1/6), 3.44 (CH-3), 1.49 (CH_3-1/6/8), 1.38 (CH_3-3)
25[k]	8.61(s)	1.91 (CH_3-3)[l]
16	—	3.63 (CH-3/6/8), 2.9 (CH-9), 2.11–1.47 (m)
19[m]	8.05	1.65 (CH_3-2), 1.58 (CH_3-7)
21[m]	7.84	1.64 (CH_3)

[a] Data for parent nitro compounds are also given in refs. 17, 19 and 20. Values in parentheses are H–H coupling constants. [b] Values are slightly different in FSO_3H·SbF_5 (4:1) or FSO_3H·SbF_5 (1:1) as solvent. [c] See also ref. 17. [d] May possibly be interchanged. [e] Broad. Resonances unresolved. [f] Assignments tentative. [g] Several weak deshielded absorptions probably belonging to minor amounts of ring protonation were also present. They subsequently disappeared when the sample was allowed to reach room temperature and then re-cooled. [h] Position depends slightly on temp. [i] Spectrum shows minor resonances probably due to ring protonation at δ 4.70 and 0.9. [j] Coupling not measured because of overlapping resonances. [k] Spectra recorded on a mixture of protonated and cyclised species. [l] Signals not discernible from those of the major cyclised form **24**. [m] Similar, but not identical to assignment in ref. 20.

152.8 was achieved by independent synthesis and protonation (FSO_3H–SO_2) of ^{15}N-labelled **1**. The ^{13}C NMR spectrum of the 15-N labelled **2** gave a doublet for the iminium carbon centred at δ 152.8 ($^1J^{13}C$–^{15}N = 29.9 Hz and $^1\Delta^{13}C^{15}N$ = 0.041 ppm; the latter value is of the right order of magnitude[21]). The remaining 15 aromatic signals were identical to those of unlabelled **2**. Comparison of the position of the iminium carbon with the C_1 absorption for diprotonated *para*-substituted nitrosobenzenes (*ca.* 145 ppm)[5] shows it to be *ca.* 8 ppm more deshielded, but 18 ppm more deshielded than the C_1 resonance of the diprotonated 1-nitronaphthalene (at 135.6 ppm).[7] The most deshielded aromatic carbon signals, at 187.5 and 183.7 ppm, are due to C-6/C-8 [HETCOR analysis (Fig. 5) and in analogy with other alkyl(cycloalkyl)pyrenium and fluoroalkylpyrenium ions].[17,18]

In the aliphatic region of **2**, there are five Pr^i(CH) signals between δ 35.2–26.2 and ten Pr^i(Me) absorptions between 26.2–19.5. No carbon resonances are found between δ 122.3–35.2 thus ruling out cyclisation (see below) or sulfinylation.[17]

Following complete cyclisation to **6**, the ^{13}C NMR spectrum shows only sixteen aromatic absorptions between δ 187.7–122.8, four Pr^i(CH) between 32.8–22.9 and four Pr^i(Me) absorptions (2:1:1:1 ratio). Comparison of the Pr^i(CH) region for the two pyrenium ions [Figs. 4(*a*), (*b*)] leads to the conclusion that the most deshielded Pr^i(CH) for **2** at 35.2 (not present in **6**) is at C-2; furthermore, HETCOR analysis confirms that the anisotropically shielded Pr^i(C*H*) at δ 3.16 is at this carbon (Fig. 5).

The notable feature is the signal at δ 87.2 for the $C(CH_3)_2$ carbon of the side chain attached to oxygen (oxazoline ring). By independent protonation and subsequent rearrangement of the resulting ^{15}N-labelled **2** it was established that the iminium carbon in the cyclised ion was the signal at δ 149.4, showing that cyclisation causes slight shielding of this carbon. The $^1J^{13}C$–^{15}N for the cyclised ion is reduced to 21.9 Hz compared with the non-cyclised ion ($^1\Delta^{13}C^{15}N$ = 0.0275 ppm). Overall, the charge distribution patterns in **2** and **6** are quite similar (Fig. 1) with the positive charge existing predominantly at alternating carbons of the periphery at the phenalenium moiety *viz.* at C–6/C–8, C–3a/C–10a and C–5/C–9, in line with the charge distribution mechanism established in alkylpyrenium and fluoroalkylpyrenium ions.[16–18]

Protonation of **1** *with 'Magic Acid'®–*SO_2; *N,N-Dihydroxyiminium–pyrenium (and oxoiminium–pyrenium) Dication Formation and Cyclisation to* **6**.—The $=N(OH)_2^+$ group of the *N,N*-dihydroxyiminium–pyrenium dication formed by protonation of 1-nitropyrene with 'magic acid'® gave two OH signals at δ 15.40 and 15.20.[12] In order to freeze out a possible dynamic proton exchange of the OH groups in **2**, **1** was treated with 'magic acid'®/SO_2 at −75 °C to give a dark-red solution, whose ^{1}H NMR spectrum (at −70 °C) showed clean generation of the *N,N*-dihydroxyiminium–pyrenium dication **2** (or **8**) (95%) with minor amounts of **6** (5%). Remarkably, the expected OH absorptions for the $=N(OH)_2^+$ group were still not detectable! No unusual broadening of the FSO_3H peak was seen. The situation encountered with **2** regarding buttressing of one *ortho*

Table 2 ^{13}C chemical shifts and $\Delta\delta$s of parent nitropyrenes[a]

	C-1	C-2	C-3	C-4	C-5	C-6	C-7	C-8	C-9	C-10	C-3a	C-5a	C-8a	C-10a	C-10b	C-10c	Sum of $\Delta\delta$s
1	144.4[f]	136.8[b]	117.9[e]	141.0	120.3	142.4	119.4	143.3	123.1	139.8	131.7	125.5	125.3	126.4[c]	121.6[d]	122.6	
	26.9	−8.3	0.4	0	2.0	0.8	0.6	1.7	4.8	−1.2	1.1	0	−0.2	−4.2	0.1	−1.1	23.4
12	144.6	144.3	144.6	124.7	124.7	139.2	121.8	139.2	124.7	124.7	124.7	122.0	122.0	124.7	—[g,h]	123.4[h]	
	27.1	−0.8	27.1	−16.5	6.4	−1.6	3.0	−1.6	6.4	−16.5	−5.9	−3.4	−3.4	−5.9	—	0.7	5.7
16	145.2	121.6	140.2	120.9	124.5	142.7	118.8	142.9	123.1	138.6	131.0	124.6	125.4	127.8	123.8[h]	125.6[h]	
	25.9	0.2	0.7	0.2	4.0	2.9	0.2	3.2	6.7	−0.6	3.8	10.6	0.2	−1.6	−3.0	0.3	43.7
19	144.9(5)[i]	136.8(5)	126.5	129.0	130.2	123.6	149.8	123.2	129.8	123.7	131.2	130.2	130.4	123.2	122.8[h]	121.4[h]	
	23.0(5)	−11.5(5)	4.6	1.7	2.9	1.7	1.4	1.3	2.5	−3.6(5)	0.5	−0.6	−0.3	−7.5	0	−1.35	14.8
23	144.3	120.9	142.3	147.7	123.5	145.7(5)	120.3	144.8(5)	122.5	121.9(5)	117.6	127.1	126.3	126.3(5)	128.1	123.5	
	2.8	2.0	0.8	26.2	2.0	4.2(5)	1.4	3.3(5)	1.0	0.4(5)	−8.5	1.0	0.2	0.2(5)	1.7	−3.1	35.8
28	142.4(5)[i]	122.4(5)[j]	123.9[h]	127.5	130.5	126.6	127.0	126.9	131.2	121.4	134.8	130.7	129.8	124.5[k,l]	124.5[l]	124.3	
	17.2(5)	−3.8(5)	−1.3	0	3.0	1.4	0.7	1.7	3.7	−6.1	3.7	−0.4	−1.2	−6.6	1.2	−1.0	12.3

[a] In $CDCl_3$. δ relative to internal TMS. [b] $J(C,N) = 1.4(5)$ Hz. [c] $J(C,N) = 2.2$ Hz. [d] $J(C,N) = 1.3$ Hz. [e] $J(C,N) = 2.1$ Hz. [f] $^1J(C,N) = 14.4$ Hz, $^1\Delta(C,N) = 0.019(5)$ ppm. [g] Not observed. [h] May be exchanged. [i] $^1J(C,N) = 14.8$ Hz. [j] $J(C,N) = 1.7$ Hz. [k] $J(C,N) = 2.45$ Hz. [l] Overlapping.

and one *peri* methyl groups and shielding of the *peri* $Pr^i(CH)$ remained unchanged [very similar $Pr^i(Me)$ region in both the ^1H and ^{13}C spectrum]. In the aromatic region, the two low field resonances showed a slightly larger separation in 'magic acid'® relative to FSO_3H (Table 1).

Whereas the absence of an independent OH absorption in 'magic acid'® at −70 °C, may suggest formation of the oxo-iminium–pyrenium cation **8**, the anticipated difficulty in intramolecular cyclisation for a 'linear' NO group as compared with $=N(OH)_2^+$ seems to argue against such a species as the predominant cation and as direct precursor to the cyclised cation **6**. Moreover, the observation of methyl group non-equivalence advocates against **8** as the direct precursor.

Close examination of the ^{13}C NMR spectrum of **2** in various superacid media with $TfOH–SO_2$ or $FSO_3H–SO_2$ or SO_2ClF provided additional clues: there are only small and specific changes in the position of the iminium carbon resonances (Fig. 2). However, a distinct difference is seen for other carbon resonances as a function of H_0 (with or without SbF_5) (Fig. 2). The carbon resonances showing sensitivity are those of C-1, C-3, C-4, C-6 and C-8. The methyl resonances show non-equivalence in all solvents, but to a slightly varying degree.

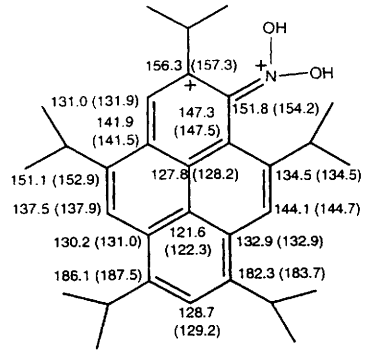

2

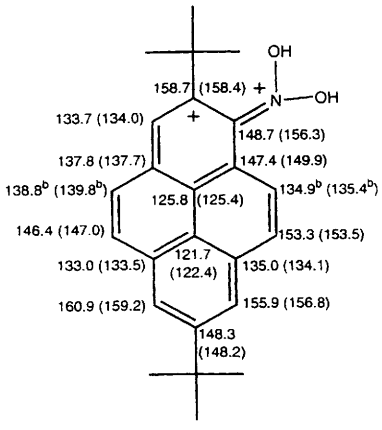

17

Fig. 2 ^{13}C chemical shifts of **2** and **20** in $CF_3SO_3H–SO_2$ and in (4:1) $FSO_3H{\cdot}SbF_5–SO_2$ (δ values in parentheses). [a] Values for $FSO_3H–SO_2$ are very similar to those of $CF_3SO_3H–SO_2$, but slightly larger. Values for $FSO_3H{\cdot}SbF_5$ (1:1)–SO_2 are similar to those of $FSO_3H{\cdot}SbF_5$ (4:1)–SO_2 or SO_2ClF, but slightly larger. [b] May be interchanged.

Quenching of **6**.—We reported[12] that quenching (ice–hydrogen carbonate) of **2** generated in $TfOH–SO_2$, gave a dark green solid (thought to be **5**), which, when redissolved in $TfOH–SO_2$, furnished cation **6** and other species (see below). We had recorded IR data on the organic extract but wished to acquire NMR data for further elucidation. Attempts to record a ^{13}C spectrum (in $CDCl_3$ or $CS_2–CDCl_3$) showed no signal from the solute! The ^1H NMR spectrum showed several weak aromatic absorptions between δ 7.50–8.60, three $Pr^i(CH)$ multiplets between 3.90–4.20 and a broad unresolved $Pr^i(Me)$. These observations pointed to the presence of a paramagnetic species, as also supported by observation of a broad EPR signal at room temperature both in $CDCl_3$ and as a solid. The paramagnetic nature of the work-up product remained unchanged on storage; the same broad EPR signal was observable in samples kept at room temp. on the bench for one month. The procedure was repeated with 64% ^{15}N enriched **2**. This caused the EPR spectrum to show both a doublet and a triplet (both broad). The yield of the work-up product was *ca.* 70% based on a fluorosulfate salt (see below). This crude fraction was separated into an ether soluble and an ether insoluble fractions. The ether soluble fraction was found to be mostly **1** and small amounts of 1,3,5,7,9-pentaisopropylpyrene together with a small impurity (TLC and ^1H NMR). This fraction is nevertheless paramagnetic according to EPR.

The ether insoluble part is clearly also paramagnetic based on NMR and EPR spectra. The latter consisted of a rather broad triplet [g = 2.005 and a_N = 8.3 G]. The ^1H NMR spectrum ($CDCl_3$ at room temp.) shows partially broadened resonances varying in both width and position in different runs. Rather sharp resonances are observed at δ 1.51 (6 H, d) and 1.61(5) (12 H, d) and at 1.62 (6 H, d). In addition there is a slightly broadened resonance found at δ 2.03 (6 H, s). Broad methine resonances are seen at 4.55, 4.2 and 3.95 ppm. A broad resonance is observed at δ 8.18 ppm (2 H) and two very

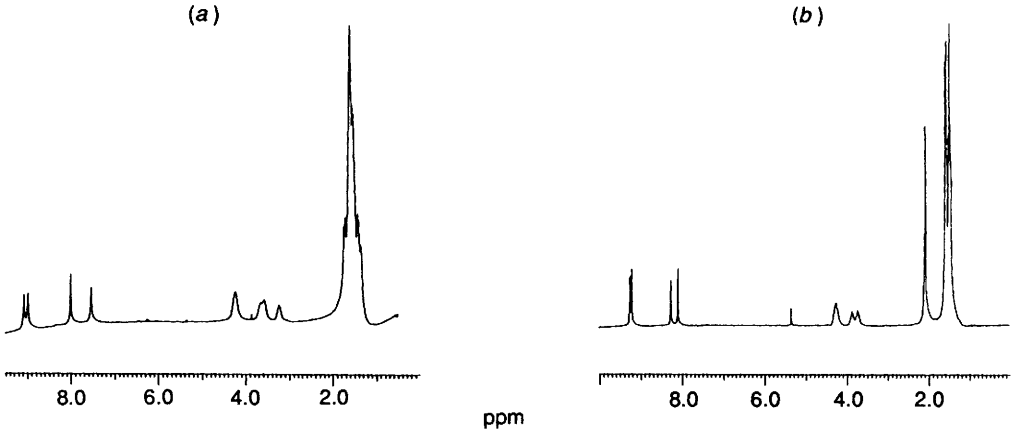

Fig. 3 ^1H NMR spectrum of (*a*) **2**; (*b*) **6**

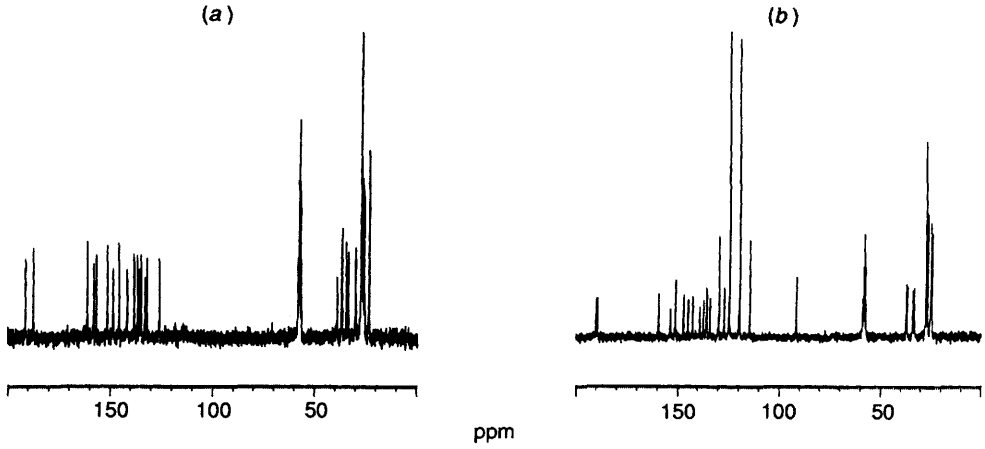

Fig. 4 ^{13}C NMR spectrum of (*a*) **2**; (*b*) **6**

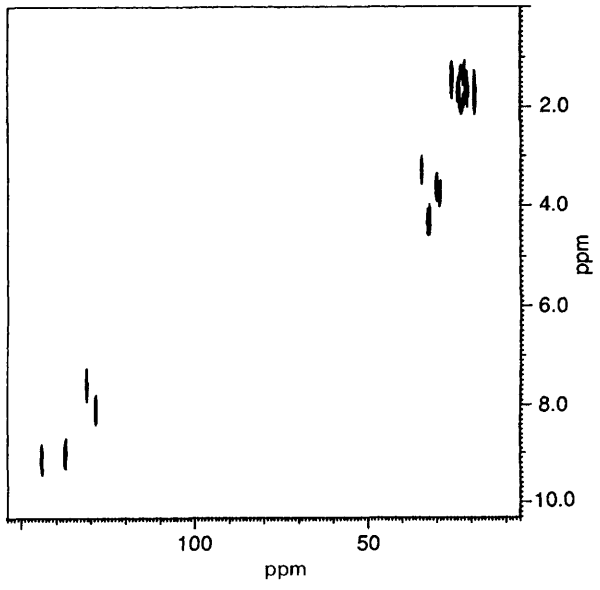

Fig. 5 ^{1}H–^{13}C heterocorrelated NMR spectrum of **2**

broad resonances barely observable at 9.1 and 9.5 ppm (1 H each). The position of the latter depends strongly on concentration of the radicals present as does the broadness of all the broad resonances.

The FAB mass spectrum gave an intense *m*/*z* 440 (base peak) and other fragment ions at 425 and 410. The corresponding EI mass spectrum showed only peaks at 425 and 410. The *m*/*z* 440 ion is compatible with structures like **6** and **9** (Scheme 1). Elemental analysis confirmed the presence of both sulfur and fluorine (see Experimental) corroborating structures like **6** and **9** (as fluorosulfate salt). However, the ^{1}H NMR spectrum is sufficiently different from that of **6** to exclude this. The IR spectrum showed no strong resonances in the 2200–2400 cm^{-1} region suggesting that the mesomeric form **9a** is predominant.

The broadness of the aromatic resonances and of resonances belonging to protons either conjugated with or in the proximity of the aromatic ring shows the presence of radicals. Since the linewidths and positions vary in the ^{1}H NMR spectra with the sample used, and all resonances can be wiped out by addition of $LiAlH(OR)_3$, it is reasonable to propose that the radical is a minor component of quenching; its structure is best compatible with **9RC** (Scheme 3).

The ether soluble fraction also gave rise to a strong, broad singlet in the EPR spectrum (g = 2.0022 and ΔH_{pp} = 13.8 G). The presence of this radical did not induce much broadening in the ^{1}H NMR spectrum of the ether soluble fraction predominantly consisting of starting material. The low g value is in accord with a structure like **9a**$^{\bullet}$.

In another experiment, **2** was generated in $TfOH–SO_2$ and allowed to rearrange at room temperature (^{1}H NMR). Cation **6** was quenched and the isolated dark green–black solid was dissolved in $TfOH–SO_2$ at low temperature to give a dark-red solution. The ^{1}H NMR spectrum of this sample (at −65 °C) showed three resonances in the 2 ppm region at δ 2.25, 2.10 and 2.05 and ten resonances at δ 8.03, 8.12, 8.22, 8.30, 9.19, 9.30, 9.40 and 9.47 (1 H each) and 8.40 and 9.25 (2 H each). These resonances seem compatible with regeneration of **6** and formation of **11** and **9** (Schemes 1–3). The ^{1}H spectrum of the latter is not identical with that just reported for **9**. This is probably due to a lower concentration of **9RC** following reaction with FSO_3H. Despite the complexity of the ^{13}C NMR spectrum of the mixture, presence of two methine carbons at δ 82 and 88 is indicative of two cyclised species in accord with **6** and **11**. When this ion mixture was quenched, a green–brown solid was isolated which was also paramagnetic. Dissolving the solid in $TfOH–SO_2$ regenerated the **6**, **9**, **11** mixture and in some cases only **6**.

Protonation of 2,4,6,8-10-*Pentaisopropyl*-1,3-*dinitropyrene* **12**.—The low temperature reaction of **12** with $FSO_3H–SO_2ClF$, $FSO_3H–SO_2$ or $TfOH–SO_2$ generates its corresponding red *N*,*N*-dihydroxyiminium–pyrenium ion **13**, for which the OH absorptions were not detectable but anisotropic shielding of two methyl doublets (*ortho* and *peri*) suggested the presence of bulky *N*,*N*-dihydroxyiminium cation substituent at C-1 (see Scheme 4).

Dication **13** cyclises readily upon raising the temperature (−78 °C ⟶ room temp.) to give **14** (dark red) as the major product. The reaction is complete within minutes. As was observed with **2**, the cyclisation barrier **13** ⟶ **14** is small, since slight excess of local overheating gives rise to rearranged product in the spectra. Thus with the more concentrated samples prepared for ^{13}C studies, **14** is already seen in the spectra (*ca.* 20%). The onset of rearrangement is easily followed, as the methyl singlet appears at δ 2.14 (6 H), concomitant with appearance of three deshielded aromatic singlets at δ 9.41, 9.33 and 8.23 (1 H each). Careful protonation at dry ice–acetone temperature with $FSO_3H–SO_2ClF$ ensures the formation of pure **13**.

The spectral appearance does not suggest a dynamic oxazoline–pyrenium species in which both *ortho* nitro groups (**1**

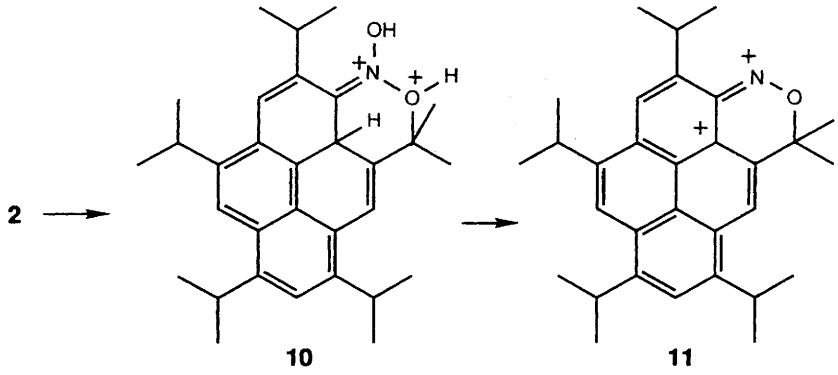

Scheme 2 Formation of the '*peri*-cyclised' ion, **11** from **2**

and **3**) participate in ring closure. Protonation/deprotonation is apparently fast on the NMR time-scale as no separate OH resonances are observed. The second nitro group cannot be protonated as diprotonation would lead to a symmetrical molecule, which is clearly not the case. This agrees with predictions based on substituent effects on **1** and **2** in both ^1H and ^{13}C NMR spectra.

Presence of a second (minor) methyl singlet at δ 2.13 and a small aromatic singlet appearing as a shoulder at δ 9.32 ppm are indications for the formation of the alternative cyclisation product (involving the *peri* Pr^i group) to give **15** as a minor product.

The ^{13}C NMR spectrum of **13** (FSO_3H–SO_2ClF at −68 °C) exhibits all of the expected sixteen aromatic signals between δ 189.7–121.7. In contrast to **2**, the aromatic region shows two resonances close to δ 120. A similar feature is found for the cyclised product, **14**. The aliphatic region exhibits four Pr^i(CH) between δ 34.5–32.0 (in a 1:2:1:1 ratio) and seven Pr^i(Me) signals between 25.7–18.7 (1:2:2:2:1:1:1 ratio) (Fig. 6).

Upon cyclisation (⟶ **14**) in FSO_3H–SO_2ClF or FSO_3H–SO_2, a diagnostic peak at δ 88.1 appears for the quaternary carbon of the side chain attached to oxygen. Dication **14** exhibits all of the expected sixteen aromatic signals between 190.0–123.0 ppm and four Pr^i(CH) absorptions. The ^{13}C NMR spectrum provides corroboratory evidence for the presence of **15** as a minor cyclisation product (smaller peaks at δ 88.3 and 122.7, and small peaks in close proximity to the individual absorptions for **14**).

Quenching Experiments on **14**.—When the FSO_3H–SO_2ClF solution of **14** was quenched a dark green solid was obtained which on standing in $CDCl_3$ turned red–brown. The ^1H NMR spectrum showed very broad Pr^i absorptions with no aromatic signals being detectable. The EPR spectrum (room temp.) exhibits a broad triplet with additional (unresolved) broadening due to coupling with the aromatic protons. Simulation (taking into account additional line broadening) gave g = 2.004 and hyperfine coupling to nitrogen, a_N = 9.0 G. In a control experiment, **13** was independently generated in FSO_3H–SO_2ClF (^1H NMR) and examined by EPR at *ca.* −70 °C. A weak absorption was seen which was broad and featureless. The sample was allowed to rearrange and examined again by EPR, the same featureless resonance but weaker in intensity was located. We conclude that the weak EPR absorption is due to a minor oxidation of the nitroalkylpyrene itself in the superacid and that the corresponding nitroso radical cation is formed on quenching.

Protonation of 3,6,8,10-*Tetracyclohexyl*-1-*nitropyrene* **16** *in* FSO_3H–SO_2ClF (*or* SO_2).—Synthesis of compound **16** provided another opportunity for examining buttressed protonated α-nitro group cyclisation to form a six-membered 1,2-oxazine-fused pyrenium ion (see Scheme 5).

Low temperature reaction of **16** with FSO_3H–SO_2ClF gave a deep red solution whose ^1H NMR spectrum is consistent with formation of **17** and minor amounts of **18**. Concomitant formation of **18** indicates that the cyclization process has a low barrier and is a facile process, similar to the isopropyl derivatives discussed earlier. The aromatic region of the ^1H NMR spectrum for each species consists of three singlets and two doublets with those belonging to **18** being the more deshielded, with the most deshielded one at δ 3.80 (2 H) is for the cyclohexyls at the C-6/C-8 positions. The most upfield cyclohexyl(CH) at 2.83 ppm disappears upon complete cyclisation and, therefore, belongs to the *peri* cyclohexyl group. The remaining cyclohexyl absorptions form a cluster between 2.10–1.40 ppm.

An identical ^1H spectrum was obtained by protonation of **16** with FSO_3H–SO_2 as solvent.

The ^{13}C NMR spectrum of **17** (at −68 °C) exhibits sixteen resonances between δ 185.3–115.4. There are four cyclohexyl-(CH) resonances between 40–46 ppm, the most upfield one of which is due to the *peri* cyclohexyl group, since this signal disappears upon cyclisation and is replaced by the carbon resonance at δ 88.8 (see below). The C–CH_2 carbon resonances of the cyclohexyl groups show non-equivalence in a similar fashion to the isopropyl groups of, for example, **2**. A change of solvent to SO_2ClF changes the relative positions of these carbons, whereas the quaternary carbons remain unchanged.

Complete rearrangement (⟶ **18**) occurs when the NMR sample is removed from the cold bath and allowed to stand at room temp. for *ca.* 5 min. A clear change in the number (and multiplicities) of the most upfield cyclohexyl resonances is seen upon cyclization. In the ^{13}C NMR spectrum of **18**, fifteen resonances are observed between 185.7–112.3 ppm in addition to a distinct cyclohexyl quarternary carbon resonance at δ 88.8. Quenching of the superacid solution of cyclised **18** produced its derived radical cation, exhibiting an intense EPR resonance which was broad and featureless. Once again, when the paramagnetic solid was redissolved in FSO_3H–SO_2, **18** was regenerated (^1H NMR). The EI mass spectrum gave a mass of 543, which, in analogy with **9**, points to a molecular weight of 559, again compatible with the fluorosulfate salt of **26** (Scheme 7, see on).

Protonation of 2,7-*Di*-tert-*butyl*-1-*nitropyrene* **19** *in* TfOH–SO_2 *and in* '*Magic acid*'®–SO_2.—The low temperature reaction of **19** with TfOH–SO_2 at dry ice–acetone temperature gave a deep-red solution. Its ^1H NMR is consistent with formation of either **20** or **20a** (see also protonation in 'magic acid'®). Indeed, under the conditions where **2** and **13** rapidly rearrange, no rearrangement of **20** (or **20a**) could be induced.

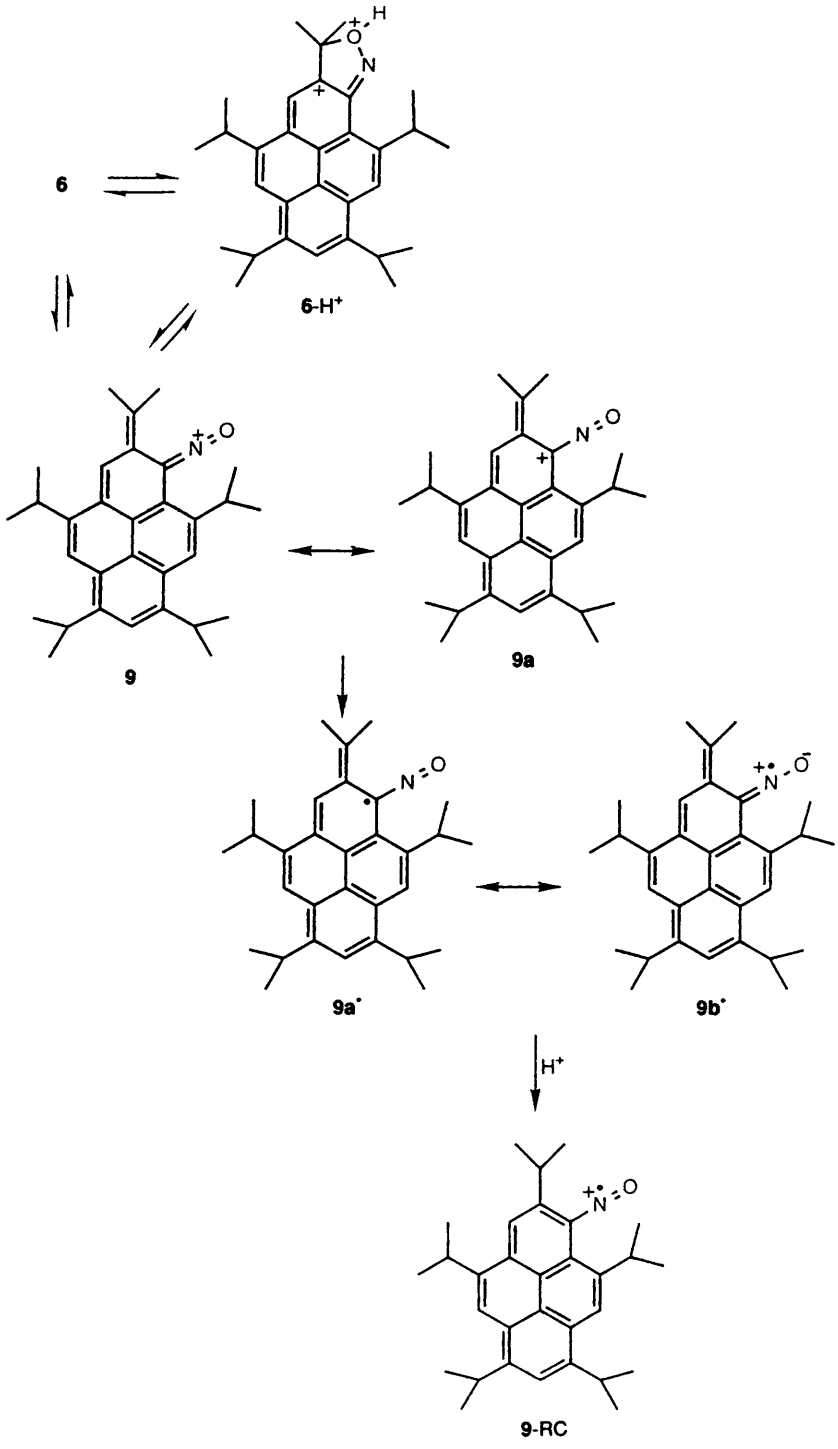

Scheme 3 The chemistry of the cyclised ions (ring opening on quenching, reduction and protonation events)

This concurs with the suggested cyclisation mechanism (see Scheme 6).

Since the OH protons were undetectable in TfOH,[12] the protonation was carried out in 'magic acid'®–SO_2ClF for comparison. The aromatic region of the ^1H NMR spectrum of the resulting red ion solution exhibits similar resonances to that obtained previously. No sp^3(CH) absorptions were observed in the spectrum and therefore no ring protonation. The aliphatic region shows one slightly broad Bu^t methyl absorption at δ *ca.* 1.53. The integral ratios confirm that no dealkylation had occurred. Thus the two Bu^t(Me) singlets coincide within the viscosity broadening range. An important feature of the spectrum is dynamic exchange involving the superacid peak which appears as a broad hump (spectrum recorded at −75 °C) centred around δ 11. Thus exchange of $=N(OH_2)^+$ protons is occurring with the solvent acid. Minor contribution by **20a** in a rapid equilibrium cannot, however, be ruled out.

Comparison between the spectral data obtained in TfOH–SO_2 with those in 'magic acid'®–SO_2ClF reveals minor differences in the position of some signals; some resonances also change position slightly.

Room Temperature Reaction of **19** *with* TfOH.—Cold TfOH was added to **19** (at *ca.* −25 °C) and the sample was mixed and allowed to reach room temperature. A dark-brown solution

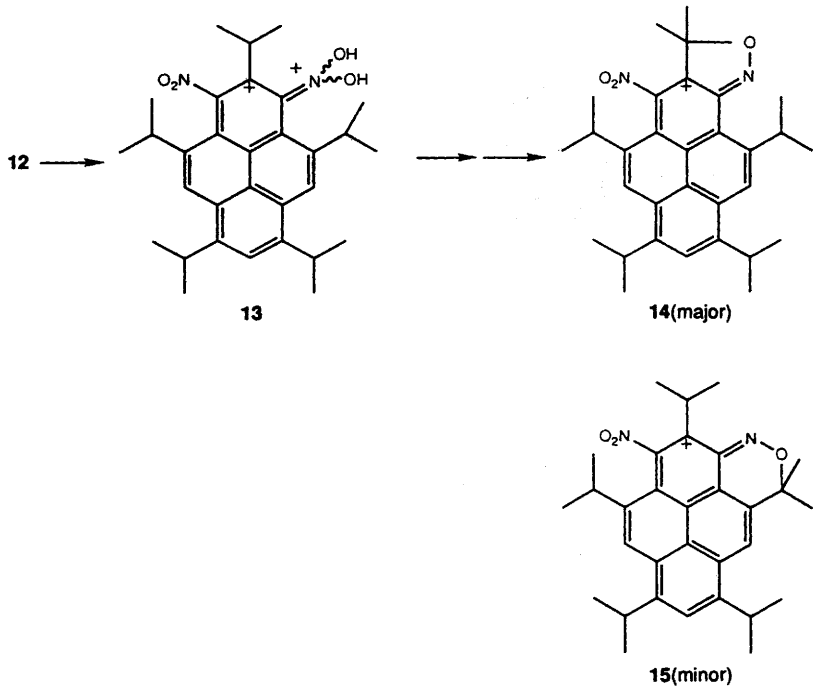

Scheme 4 Protonation and cyclisation of 2,4,6,8,10-pentaisopropyl-1,3-dinitropyrene (**12**)

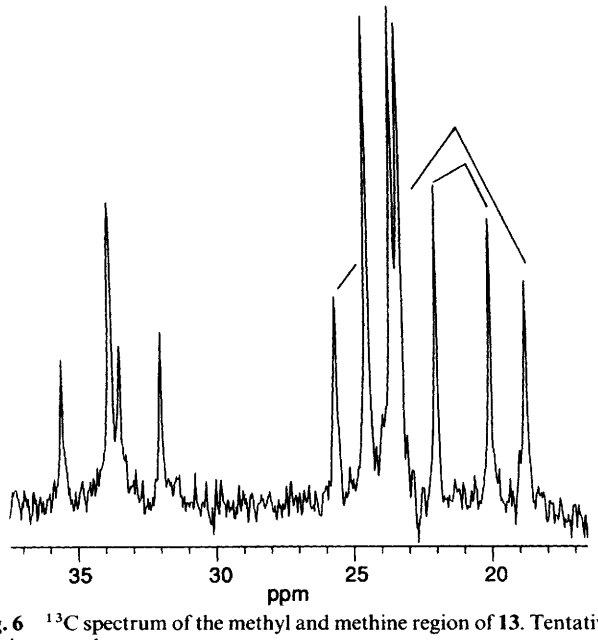

Fig. 6 ^{13}C spectrum of the methyl and methine region of **13**. Tentative pairings are shown.

resulted, the ^1H NMR spectrum of which exhibited very broad features, namely aromatic resonances between 9.50–7.80 ppm and broad Bu^t absorptions. The EPR spectrum of the sample exhibited a strong, featureless, signal with $g = 2.003$ and $\Delta H_{pp} = 8.7$ G. It is suggested that this may be due to the nitroso radical cation. Subsequent quenching and dissolution of the organic residue in $CDCl_3$ gave a red–brown solution, which was still paramagnetic (the same EPR signal). In spite of this, a well resolved ^1H NMR spectrum could be obtained for the reaction mixture, exhibiting two Bu^t singlets at 1.85/1.84 (1:1), four (1 H) doublets at 8.30, 8.22, 8.04 and 7.92 ppm and 3 (1 H) singlets at δ 8.38, 8.27 and 8.17 indicative of an α-substituted 2,7-di-*tert*-butylpyrene product. The nature of the substituent was supported by a GC–MS analysis as the nitroso-derivative.

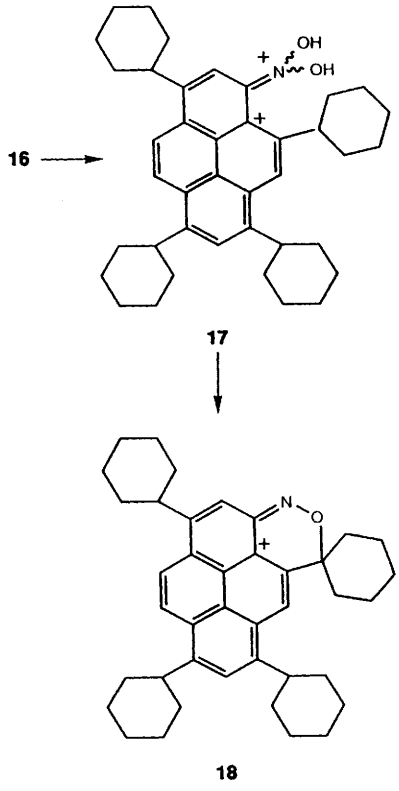

Scheme 5 Protonation and cyclisation of 3,6,8,10-tetracyclohexyl-1-nitropyrene (**16**)

Protonation of 2,7-*Di*-tert-*butyl*-1,8-*dinitropyrene* **21** *with* $TfOH–SO_2$ *or with* $FSO_3H{\cdot}SO_2$.—The ^1H NMR spectrum of the resulting red ion solution formed by reaction of **21** with $TfOH–SO_2$ (dry ice–acetone temperature) (see Scheme 6) exhibits four doublets and two singlets between 9.54–7.84 ppm (1 H each) and two Bu^t(Me) singlets at δ 1.6 and 1.55. There are also several small broad aromatic peaks mostly overlapping with the peaks due to the major cation and a broad peak at δ 4.41. The spectral data are consistent with the formation of **22a** or **22b** as the major product and a ring protonated pyrenium ion

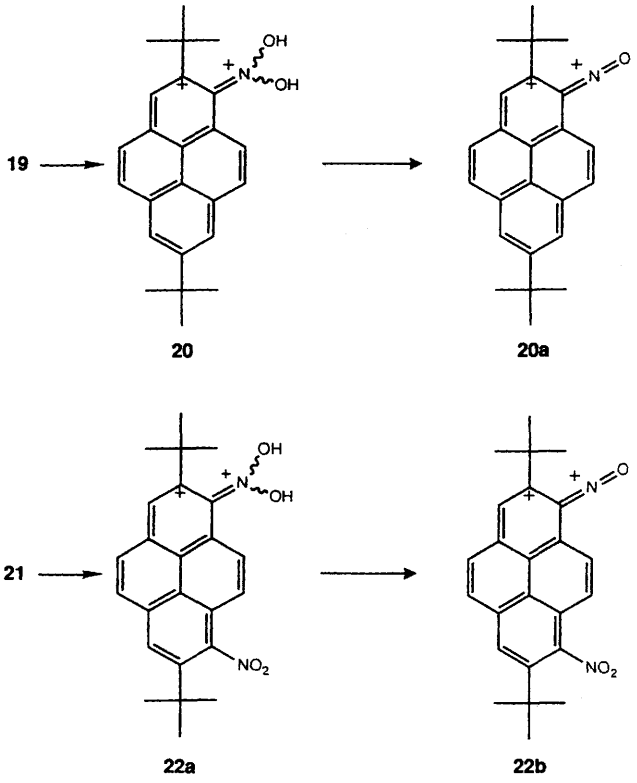

Scheme 6 Protonation of 2,7-di-*tert*-butyl-1-nitro- and 1,8-dinitropyrene (**19** and **21**)

as a minor species. The symmetry of the spectrum clearly excludes diprotonation of both nitro groups as discussed for **12**.

Protonation of 1,3,6,8-*Tetraisopropyl*-4-*nitropyrene* **23** *with* TfOH–SO_2 *and* '*Magic acid*'®–SO_2.—In compound **23** the nitro group at C-4 experiences buttressing due to *peri* Pr^i group at C-3 (Scheme 7). Low temperature protonation of **23** with TfOH–SO_2 gave a red solution whose ^1H NMR spectrum indicated the formation of two pyrenium ions (*ca.* 3:1 ratio). In the aromatic region (between δ 9.10 and 7.7), each pyrenium ion exhibits four singlets (1:1:2:1 ratio). The most upfield pair of singlets for the minor cation are barely resolved. Except for the most deshielded singlets, the remaining singlets of the minor ion are more downfield of the respective resonances of the major cation.

Four Pr^i(CH) absorptions (broad multiplets) between δ 4.2–3.4, a broad Pr^i(Me) signal and a distinct deshielded methyl singlet at δ 1.91 are observed. The last confirms that the minor cation is **25**. This is corroborated by the presence of a distinct carbon resonance at 86.5 for the quaternary carbon attached to oxygen. The major ion exhibits sixteen signals between δ 206.2 and 116.2. All the aromatic resonances of the minor ion were discernible in the spectrum (Fig. 1). The aliphatic region exhibits four Pr^i(CH) resonances between δ 36.0–29.4 and four Pr^i(Me) signals between δ 22.9–21.5 ppm (1:1:1:1 ratio). The NMR data are compatible with formation of **24** as the major and its cyclised version **25** as the minor cations respectively. Formation of **24** and its rearrangement cation was also observed in 'magic acid'®–SO_2 (a dark green solution) with minor amounts of sulfonylation σ-complexes also being present whose deshielded aromatic resonances overlapped with those of **24** and **25**.

Room Temperature Reaction of **23** *with* TfOH.—Reaction of **23** with TfOH at room temperature gave a dark-red solution. After 12 h, the ^1H NMR spectrum of the sample showed a complex mixture of pyrenium ions (aromatic absorptions between 9.60–8.0 ppm). The EPR spectrum (Fig. 7) of the TfOH solution at 297 K exhibited a rather sharp, intense septet signal [g = 2.0030; a_H = 5.13 G]. Ring opening (⟶ **26**) and reduction (⟶ **27**) produce a highly delocalised nitrosopyrene radical (lower a_N) to which the canonical form **27a** is expected to be only a minor contributor (Scheme 7).

Protonation of the Parent 1-*Nitropyrene* **28**.—Based on ^1H NMR studies,[12] we showed that protonation of **28** in 'magic acid'®–SO_2 gave the dihydroxyiminium–pyrenium dication **29**, whereas **30** was ring protonated. The present study included a ^{13}C study of **28** for comparison with other nitroalkylpyrenes reported here. The ^{13}C NMR spectrum of **28** dissolved in 'magic acid'®–SO_2 clearly shows that **29** is formed (Fig. 1).

Discussion

A Comparative Discussion of the Protonation of Sterically Crowded Nitroalkylpyrenes.—We have demonstrated that with the buttressed alkylnitropyrene substrates examined, iminium–pyrenium dication formation occurs. Steric inhibition to delocalisation (nitro group twisting) in these models is caused by bulky Pr^i and Bu^t groups placed in the *ortho* and/or *peri* positions.

Nitro group diprotonation occurs in TfOH for parent **28** and for 1-nitronaphthalene[7] (see discussion), whereas **30** is ring protonated.[12,7]

Both conjugation and steric hindrance seem important in determining the position of substitution and the type of arenium ion to be formed. The presence of nitro groups at poorly conjugated ring positions will lead to ring-protonation (2-nitropyrene). Nitro groups at well conjugated positions, but in smaller aromatic systems will be mono-protonated (nitrobenzenes) as the second charge due to diprotonation cannot be effectively delocalised. However, nitro groups at positions with good conjugation and linked to large aromatic systems (α-positions of pyrene) will be diprotonated.

The initially twisted nitro group must be able to undergo a geometrical change on diprotonation which leads to significant overlap between the developing p-orbital at nitrogen and the arene π-system. It appears that steric inhibition to delocalisation in nitro-PAHs is one of the driving forces for nitro group diprotonation in superacids, which would allow subsequent coplanarity and extensive charge delocalisation. Eventually, strong steric hindrance may support the formation of the oxoiminium cations.

The charge delocalisation as described by the sum of $\Delta\delta$'s between the charged species and the hydrocarbon precursor shows values above 200 ppm for **2**, **6**, **13**, **14**, **17**, **18**, **20** and **29** (Fig. 1), showing that the cyclised species are arenium ions. Furthermore, the sum of $\Delta\delta$'s greater than 160 ppm clearly indicates that slightly more than one charge is present on the ring. This is not caused by the use of the hydrocarbons as reference in obtaining the $\Delta\delta$ values, as the nitro group gives only a small overall substituent effect (as seen from Table 2). The extra deshielding supports the notion that the protonated and rearranged ions are in better conjugation with the ring system than the unprotonated nitro groups. However, the diprotonated 1-nitronaphthalene[7] gave only a sum of *ca.* 50 ppm according to our calculations. This casts some doubt on the formation of a diprotonated 1-nitronaphthalene under the conditions used.

The overall mode of charge distribution in the resulting dications (as probed by ^{13}C and ^1H NMR analysis) is similar to those of alkylpyrenium, cycloalkylpyrenium and fluoro(alkyl)-pyrenium ions,[16–18] showing positive charge delocalisation away from the site of attack at alternating carbon of the

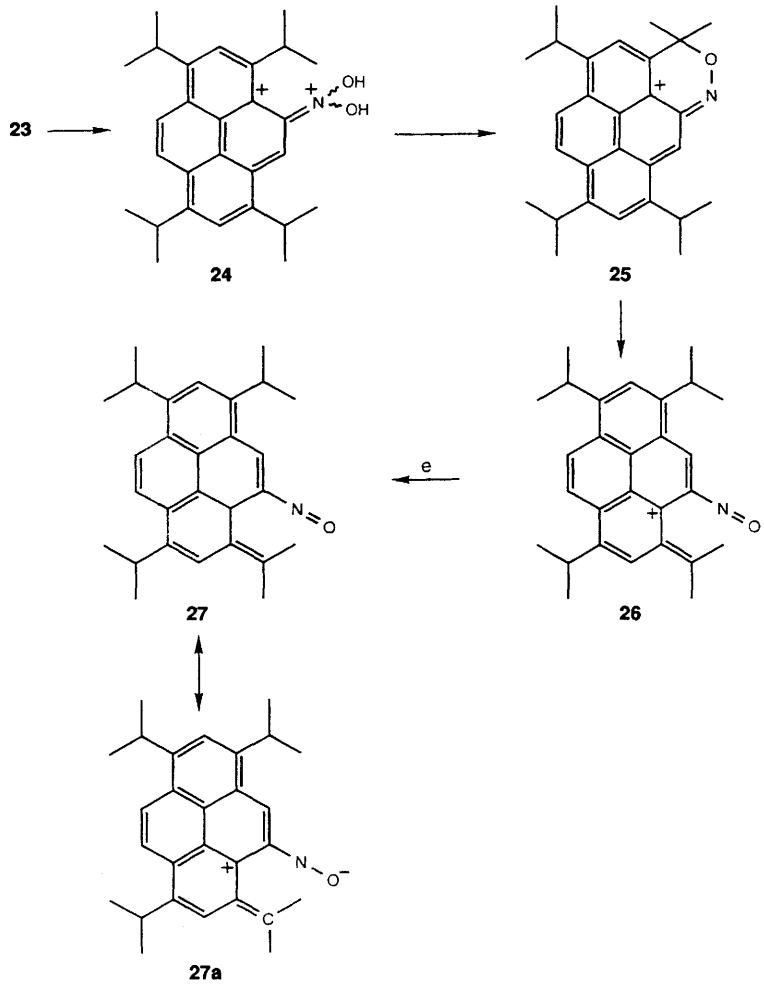

Scheme 7 Protonation and cyclisation of 1,3,6,8-tetraisopropyl-4-nitropyrene (**23**)

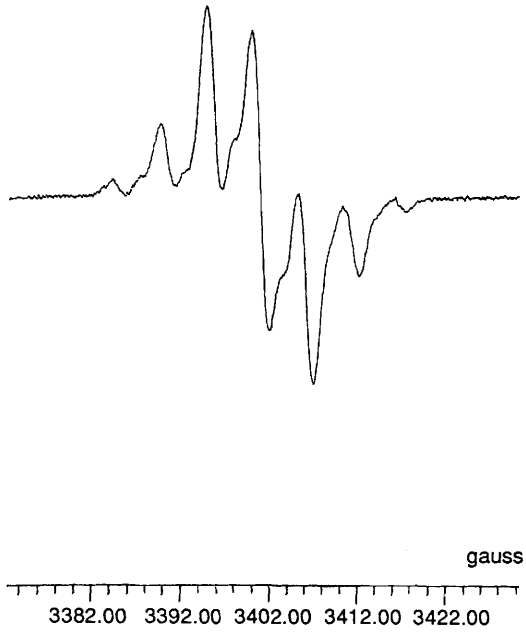

Fig. 7 The EPR spectrum of **27**

periphery. Therefore, the phenalenium ion character of α-iminium–pyrenium dications and phenanthrenium character of αβ-iminium–pyrenium dications are revealed (Fig. 1). We find that for iminium–pyrenium dications as well as their cyclised analogues more positive charge is sustained at the 'remote' α carbon of the periphery as compared to alkyl(fluoroalkyl)-pyrenium ions.[17,18] The extent of positive charge present at the 'remote' α positions is modulated by the inductively stabilising substituents, increasing further when Pr^i groups are placed at these positions.

In general, protonation occurs at nitro groups in α-positions. In **23**, NO_2 protonation can also be achieved, rendering **23** a unique case for studying charge delocalisation from an αβ-position. The positive charge delocalisation is extensive as judged from the very large positive effects (Fig. 1).

The chemical shift and charge delocalisation patterns are similar for diprotonated α-substituted nitropyrenes and their cyclised derivatives to those observed for ring protonated pyrenium ions.[17,18] As a consequence, we can expect these to be general.

It is not trivial to distinguish *N,N*-dihydroxyiminium and oxoiminium structures in TfOH–SO_2 or in FSO_3H–SO_2ClF solvents, where dynamic proton exchange involving $=N(OH)_2^+$ and the superacid is expected. However, anisotropic shielding of the *ortho* and *peri* Pr^i(Me) groups, which reflects the presence of the bulkier $=N(OH)_2^+$ group (as compared with $=NO^+$), and comparison of the NMR data with those of protonation in 'magic acid'®–SO_2 (or SO_2ClF) provided reasonable clues: the diprotonated nitro group of **2** causes non-equivalence of the methyl groups of the isopropyl groups at C-2 and C-10 in the ^1H spectrum. In the ^{13}C spectrum, four isopropyl groups have non-equivalent methyl groups. The pairing is tentative. For three isopropyl groups a considerable chemical shift difference of *ca.* 3 ppm exists between methyl resonances belonging to the same isopropyl group. For the cyclised compound (**6**) non-equivalence is no longer observed. For the diprotonated dinitro compound, **13**, the picture is slightly different (Fig. 6). The ^1H spectrum shows only two isopropyl groups with non-equivalent isopropyl groups and the same is true of the ^{13}C spectrum. For the cyclised compound, **14**, both ^1H and ^{13}C spectra show one isopropyl group with non-equivalent methyl groups; **17** shows non-equivalent C–CH_2 carbon resonances. Interestingly, **24** does not show non-equivalent isopropyl methyl groups neither do any of the parent nitro compounds. The planar oxazoline ring, as formed in **6** and **14** does not cause non-equivalence of the methyl group chemical shifts of neighbouring isopropyl groups. A similar situation is found for **18** with respect to the methylene carbons. The $=N^+=O$ is linear and even less space filling than the oxizaline ring system. We can hence assume that this will also not give rise to non-equivalence. The non-equivalence could possibly be caused by non-planarity of the molecule due to steric strain.[22,23] The non-equivalence appears to be an excellent way to distinguish the dihydroxyiminium and the oxoiminium ions.

The expanded mechanism (Schemes 1 and 2) provides a satisfactory explanation for the cyclisation of persistent dihydroxyiminium–pyrenium dications.

Formation of the six-membered 1,2-oxazines involving the *peri*-cyclohexyl (or Pr^i) groups may be explained by 1,3-hydride shift, ring closure and dehydration events. Similar arguments are applicable to ring closures involving oxoiminium pyrenium dications.

Five-membered ring oxazolines are formed more easily than six-membered 1,2-oxazines (formation of **6** rather than **11**). Formation of **11** is probably less favoured as it involves intermediates like **10**, in which ring protonation occurs at a non α-position (Scheme 2). In case of **13**, both **14** (major) and **15** (minor) are formed when the temperature was raised. The steric hindrance between the $(CH_3)_2$ group and the second nitro group could destabilise **13**. For **24**, the cyclisation reaction is clearly less favoured as a number of side products appear upon prolonged treatment as well as on formation of **24** in 'magic acid'® solvent. We find that the iminium–pyrenium cations derived from *tert*-butylnitropyrenes do not rearrange under the conditions where the Pr^i- and cyclohexyl-substituted analogues do.

The data given in Fig. 1 are normally recorded in FSO_3H–SO_2 or CF_3SO_3H–SO_3 systems. From Fig. 2 it is seen that ^{13}C NMR data obtained in SbF_5 containing superacids in SO_2ClF [FSO_3H·SbF_5 (4:1) or (1:1)] show further low field shifts primarily at the carbon carrying the protonated nitro group. As non-equivalence of the methyl groups for **2** is observed in all solvents, we conclude, that the diprotonated species (**2**) is dominating and that the enhanced deshielding is caused by counterion stabilisation (lower gegenion nucleophilicity). A similar argument is valid for **20**.

According to Scheme 1, ring closure requires the formation of **3**. Judging from the C-1 chemical shifts, this is only present in very small amounts. Subsequent reactions eventually leading to cyclised ions are also fast on the NMR time-scale.†

The present studies provide new insight into the behaviour of cyclised cations **6**, **15** and **18**, which on quenching form alkyl(cycloalkyl)nitrosopyrenium together with its *in situ* reduced radical cations, from which the original cyclised cation may be generated by reaction with TfOH or FSO_3H. The extreme stability of nitroso salts like **9** (as fluorosulfate) and its radical cation **9RC** are to our knowledge unprecedented. Formation of **9** as a crucial intermediate and its redox chemistry in superacid media provide a satisfactory explanation for our observations.

Experimental

Triflic acid 'TfOH', fluorosulfonic acid FSO_3H (Linde or Aldrich) and SbF_5 (Fluorochem or Aldrich) were all doubly distilled at atmospheric pressure under dry nitrogen and stored in Nalgene bottles. SO_2ClF (Aldrich) and SO_2 (Linde, anhydrous) were used without additional purification. The preparation of the superacid solutions were analogous to our previously published procedures.[24] Persistent cations were generated using the procedures already described.[16–18] $Na^{15}NO_3$ (64%) was purchased from Isotec.

The NMR spectra were recorded on a GE/GN-300 and a Bruker AC 250 spectrometer. Details of the low temperature NMR techniques and procedures have been given.[16–18,25] The chemical shifts are referenced to CH_2Cl_2 (using CD_2Cl_2 as internal reference). For hetero correlated spectra the sweep width was 2500 in F_1 (^1H) and 17 857 Hz in F_2 (^{13}C). The 2D spectra were collected in 128 × 2048 data matrices and sine bell apodisation was used in F_1. The FIDs were zero filled to 512 times 2048 words before transformation. The pulse sequence was optimised for a one-bond coupling of 150 Hz. 32 scans were measured for every increment.

X-Band EPR spectra were obtained using an IBM-200D-SRC spectrometer with an ER 4111 temperature controller (1 K precision).

The organic residue obtained upon quenching of the superacid solutions was dissolved in $CDCl_3$ (*ca.* 12 mg in 1 cm^3 of solvent), an aliquot was transferred *via* a pipette into a Wilmad quartz EPR tube under argon. The sample was repeatedly flushed with argon under vigorous stirring and sealed. The EPR spectra of the superacid solution were recorded by transferring a cold aliquot from a 5 mm NMR tube into a Wilmad quartz tube under argon. These were examined between −70 and −40 °C.

Infrared spectra were recorded on a Perkin-Elmer 1710 FT spectrometer.

FAB mass spectra were obtained on a Kratos MS 50 TC

† An equilibrium between dihydroxyiminium and oxoiminium species cannot be significant in superacids, since the back reaction requires nucleophilic attack by water. Equilibrium involvement of the sulfate ester of dihydroxyiminium cation (FSO_3^- or $CF_3SO_3^-$ as nucleophiles) may be considered, but quenching of oxoiminium ion with such low nucleophilicity counter ions especially in 'magic acid'® at low temperature is not envisaged nor is there any NMR evidence for the existence of these highly crowded derivatives.

instrument. The GC–MS spectra were obtained on a Hewlett Packard 5890 Gas Chromatograph equipped with a 5971A Mass Spectrometer.

The elementary analysis was done by National Chemical Consulting, Tenafly, NJ.

Compounds **1**, **12**, **13** and **23** were available from our previous study.[12]

Compounds **19** and **21** were synthesised by classical protic nitration of 2,7-di-*tert*-butylpyrene.[20] Typically, the substrate (1 g, *ca.* 3.2 mmol) was dissolved in warm glacial acetic acid (*ca.* 25 cm^3) and a mixture of conc. HNO_3 and glacial acetic acid (1:10) was then added to give a substrate to HNO_3 molar ratio of 1:0.9. The reaction mixture was allowed to stand for 10 min and subsequently cooled (crushed ice) and water was added. The precipitate was filtered and the crude organic product mixture (0.8 g, *ca.* 78%) was subjected to TLC analysis showing **19** together with three isomeric dinitro-derivatives namely the 1,8- (**21**), the 1,6- and the 1,3-dinitro compounds. Compounds **19** and **21** were purified by column chromatography (silica gel; particle size 0.063–0.200 mm) using hexane–chloroform (4:1, *v*/*v*): 2,7-di-*tert*-butyl-1-nitropyrene **19** (mp 168.7–169.4). The 2,7-di-*tert*-butyl-1,8-dinitropyrene **21** (mp > 300 °C).

Quenching experiment on **19**. The NMR tube containing the protonated substrates (usually in TfOH) carefully poured into ice–hydrogen carbonate (efficient mixing). The organic residue was taken up into $CHCl_3$ and dried ($MgSO_4$). The red–brown compound gave a GC–MS with a base peak at *m*/*z* 329, and important fragment ions at *m*/*z* 314 (loss of Me), 258 (loss of Bu^t), 217 and 207.

Synthesis of ^{15}N-*labelled* **1**. This was prepared by nitration of the corresponding alkylpyrene by dissolving $Na^{15}NO_3$ (64%) in HOAC.

Synthesis of **16**. 1,3,6,9-Tetracyclohexylpyrene was nitrated with 1 equiv. of HNO_3 in glacial acetic acid. The crude product was purified by flash chromatography on silica gel. Mp 278. The MS (EI) gave an $M^{\bullet+}$ at 575 and a strong peak at 558, characteristic of a loss of 17 (OH) also found for 1,3,6,8-tetraisopropyl-4-nitropyrene:[12] ν_{max}(KBr)/cm^{-1} 2930 (s), 2854 (m), 1611 (w), 1528br (m), 1450 (m), 1349br (m), 999 (w) and 879 (m); λ_{max}(EtOH)/nm 248.5, 290.5, 351.7 and 433.9. **9**: *m*/*z* (FAB) 440, 425 and 410; *m*/*z* (EI) 425 and 410; ν_{max}(KBr)/cm^{-1} 2965 (s), 2930 (m), 2871 (w), 1647 (m), 1610 (m), 1581 (m), 1530 (m), 1478 (s), 1392 (m), 1276 (s), 1261 (m), 1056 (m), 712 (m) and 579 (m). Anal. calc. for $C_{31}H_{38}NO_4FS$ (539): C, 69.02; H, 7.05; F, 3.52; N, 2.60; O, 11.87; S, 5.94. Found: C, 68.1; H, 7.2; F, 3.4; N, 2.3; S, 6.0%.

Acknowledgements

We thank Drs. Edward Gelerinter (Physics Dept., KSU) for recording the EPR spectra and Jens Arne Pedersen (Århus University) for advice, Drs. Jørgen Møller (Chemistry Dept., University of Odense) and Helge Egsgaard (Risø National Lab.) for recording the mass spectra, and Professor Arne Berg for some of the samples.

Partial support was provided by the Danish Natural Science Council (Visiting Professorship to K. K. L. at Roskilde) and NATO (CRG 930113). We also thank KSU for support and the Ohio academic challenge program for the purchasing funds for a GE/GN-300 NMR instrument.

References

1 R. J. Gillespie, *J. Chem. Soc.*, 1950, 2542.
2 N. C. Deno; R. W. Gaugler and M. J. Wisotsky, *J. Org. Chem.*, 1966, **31**, 1968.
3 G. A. Olah and T. E. Kiovsky, *J. Am. Chem. Soc.*, 1968, **90**, 6461.
4 G. A. Olah and A. P. Fong, *J. Org. Chem.*, 1980, **45**, 4149.
5 G. A. Olah and D. J. Donovan, *J. Org. Chem.*, 1978, **43**, 1743.
6 T. Ohta, K. Shudo and T. Okamoto, *Tetrahedron Lett.*, 1977, **25**, 101.
7 T. Ohta, K. Shudo and T. Okamoto, *Tetrahedron Lett.*, 1984, **25**, 325.
8 J.-M. Coustard, J.-C. Jacquesy and B. Violeau, *Tetrahedron Lett.*, 1992, **33**, 8085.
9 J.-M. Coustard, J.-C. Jacquesy and B. Violeau, *Tetrahedron Lett.*, 1991, **32**, 3075.
10 C. Berrier, R. Brahmi, H. Carreyre, J.-M. Coustard and J.-C. Jacquesy, *Tetrahedron Lett.*, 1989, **30**, 5763.
11 C. Berrier, R. Brahmi, H. Carreyre, J.-M. Coustard, J.-C. Jacquesy and B. Violeau, *Bull. Soc. Chim. Fr.*, 1991, **128**, 730.
12 K. K. Laali, T.-M. Liang and P. E. Hansen, *J. Org. Chem.*, 1992, **57**, 2658.
13 T. Ohwada, M. Kasuga and K. Shudo, *J. Org. Chem.*, 1990, **55**, 2717.
14 (*a*) J. V. Bullen, J. H. Ridd and O. Sabek, *Gazz. Chim. Ital.*, 1990, **120**, 291; (*b*) J. V. Bullen, J. H. Ridd and O. Sabek, *J. Chem. Soc., Perkin. Trans. 2*, 1990, 1681.
15 (*a*) R. P. Austin and J. H. Ridd, *J. Chem. Soc., Perkin Trans. 2*, 1993, 1229; (*b*) R. P. Austin and J. H. Ridd, *J. Chem. Soc., Perkin Trans. 2*, 1994, 1411.
16 K. K. Laali and P. E. Hansen, *J. Org. Chem.*, 1991, **56**, 6795.
17 K. K. Laali and P. E. Hansen, *J. Org. Chem.*, 1993, **58**, 4096.
18 K. K. Laali and P. E. Hansen, *J. Chem. Soc., Perkin Trans. 2*, 1994, 2249.
19 A. M. van-den Braken-Leersum, C. Tintel, M. van't Selfde, J. Cornelisse and J. Lugtenburg, *Recl. Trav. Chim. Pays-Bas.*, 1987, **106**, 120.
20 L. Rodenburg, R. Brandsma, C. Tintel, J. van Thuilj, J. Lugtenburg and J. Cornelisse, *Recl. Trav. Chim. Pays-Bas.*, 1986, **105**, 156.
21 C. Bremard, B. Mouchel and S. Sueur, *J. Chem. Soc., Chem. Commun.*, 1982, 300.
22 I. R. Gault, W. D. Ollis and I. O. Sutherland, *J. Chem. Soc., Chem. Commun.*, 1970, 269.
23 W. B. Jennings, *Chem. Rev.*, 1975, **75**, 307.
24 K. K. Laali, G. F. Koser, S. Subramaniyam and D. A. Forsyth, *J. Org. Chem.*, 1993, **58**, 1385.
25 K. K. Laali, P. E. Hansen, E. Gelerinter and J. J. Houser, *J. Org. Chem.*, 1993, **58**, 4088.

Paper 4/06324D
Received 17*th October* 1994
Accepted 11*th November* 1994